PAPER

Length-scale competition in the parametrically driven nonlinear Dirac equation with a spatially periodic force

IOP Publishing Journal of Physics A: Mathematical and Theoretical

J. Phys. A: Math. Theor. **52** (2019) 285201 (16pp) https://doi.org/10.1088/1751-8121/ab2469

Length-scale competition in the parametrically driven nonlinear Dirac equation with a spatially periodic force

Niurka R Quintero[1,5], Bernardo Sánchez-Rey[1], Fred Cooper[2,3] and Franz G Mertens[4]

[1] Departament of Applied Physics I, E.P.S. University of Seville, 41011 Seville, Spain
[2] Santa Fe Institute, Santa Fe, NM 87501, United States of America
[3] Theoretical Division and Center for Nonlinear Studies, Los Alamos National Laboratory, Los Alamos, NM 87545, United States of America
[4] Physikalisches Institut, Universität Bayreuth, D-95440 Bayreuth, Germany

E-mail: niurka@us.es, bernardo@us.es, cooper@santafe.edu and franzgmertens@gmail.com

Received 16 March 2019
Accepted for publication 24 May 2019
Published 14 June 2019

Abstract

Soliton dynamics in the damped and parametrically driven nonlinear Dirac equation, in $1+1$ dimension with scalar–scalar self-interaction is analysed. The considered parametric force has the spatial period λ. A variational approach using collective coordinates for studying the time dependent response of the solitary waves to this parametric force is developed. The dynamical equations for the collective coordinates are also obtained by an alternative method, namely the method of moments. The soliton dynamics depends crucially on the competition between two length scales: the spatial period λ and the width of the soliton l_s. For $\lambda \gg l_s$ the soliton oscillates in an effective potential, while for $\lambda \ll l_s$ it moves uniformly as a free particle. The transition between these two regimes occurs when λ is comparable to the soliton width. This match enhances the soliton instabilities so that even small values of the perturbation are enough to modify drastically the soliton shape and destroy it for long times.

Keywords: two-component spinors, parametric force with damping, collective coordinates

(Some figures may appear in colour only in the online journal)

[5] Author to whom any correspondence should be addressed.

1. Introduction

Non-topological solitons and envelope solitons are nonlinear waves represented by localized pulses in space that travel with a permanent shape, and interact elastically with other nonlinear waves [1]. The nonlinear Schrödinger (NLS) and the nonlinear Dirac (NLD) equations possess these types of solutions, which depend on parameters such as the soliton velocity and the soliton width, among others [2]. In the case of topological solitons (kinks) of sine-Gordon, double sine-Gordon or φ^4 equations, their widths are related to the spatial localization of the energy density [3].

Under certain perturbations the solitons behave as particles with a variable mass and its dynamics can be reduced to the study of the evolution equations of a few degrees of freedom, the so-called collective coordinates [2, 4]. The variable mass is closely related to the soliton width. This is the case, for instance, of NLD and NLS solitons with external perturbations [5, 6], of the kinks in the damped driven sine-Gordon, double sine-Gordon and φ^4 equations [7, 8], and of the domain walls along a helix-shaped nanowire in the Landau–Lifshitz equation [9]. The oscillations of the width of the soliton, together with the evolution of the other collective coordinates, allow to explain: (i) the propagation of the pulses in a dispersion-shifted optical fiber with dissipation, higher-order dispersion, Raman scattering, and self-steepening perturbations [10]; (ii) the mechanism underlying the net motion of fluxons in the Josephson junctions driven by a biharmonic current. The articles [7, 11] show that although the driven current has a zero average, due to the oscillations of the soliton width the center of the soliton feels an effective force with a time average different from zero; (iii) the motion of magnetic walls in curved nanostripes [12]; (iv) the length-scale competition in parametrically driven soliton-bearing equations [13].

This latter phenomenon was observed when a spatially periodic parametric force proportional to $\cos(Kx)$ is introduced in the sine-Gordon, in the φ^4, and in the NLS equations [14–16]. The length-scale competition appears when the soliton width is comparable with the period $\lambda = 2\pi/K$. In this case, the dynamics of the soliton drastically changes and is very sensitive to the specific details of the system under study. For instance, in [17, 18] it is found that the sine-Gordon breather splits into kink-antikink pairs, while in [15] the NLS soliton destabilizes and breaks up into smaller localized excitations and radiation. Moreover, for the sine-Gordon kinks, when the width of the soliton is much smaller or much larger than λ, it was shown [16] that the soliton behaves as a particle in the presence of an effective potential.

In the NLD equation the effect of various external forces on the soliton dynamics has been investigated [19–21], however parametric driving has not been considered so far. Therefore the length-scale competition in the NLD equation has not been addressed. For this reason, the aim of the current work is precisely to study the dynamics of solitary waves in the damped NLD equation with a parametric force proportional to $\cos(Kx)$. In order to achieve this goal, first in section 2, both this force and the damping are introduced in the NLD equation, and dynamical equations for the charge, the momentum and the soliton energy are derived. In section 3, an ansatz with five collective coordinates is used as an approximate solution of the parametrically driven NLD equation, and the equations of motion for the collective coordinates are obtained. Then, in section 4, simulations of the NLD equation are discussed and compared with numerical solutions of the collective coordinates equations. As the wavenumber K is progressively increased from zero, the length-scale competition phenomenon appears, destabilizing the soliton and giving rise to a transition between oscillatory and net motion. Finally, the main results of the work and the conclusions are summarized in section 5.

2. Damped and parametrically driven NLD equation

The parametrically driven, damped NLS equation for a complex field $u(x,t)$ was considered in [22, 23]. There, a parametric driving was introduced through the term $h(x,t)u^\star(x,t)$ and the dissipation through the term $-\mathrm{i}\rho u(x,t)$. Analogously, the parametrically driven and damped NLD equation is given by

$$\mathrm{i}\gamma^\mu\partial_\mu\Psi - m\Psi + g^2(\bar\Psi\Psi)\Psi = f(x)\Psi^\star - \mathrm{i}\,\rho\,\gamma^0\,\Psi\,, \tag{1}$$

where m is the mass, g is a nonlinear coupling constant, γ^0 and γ^1 are Dirac matrices related with the Pauli matrices σ_2 and σ_3 [24]

$$\gamma^0 = \sigma_3 = \begin{pmatrix} 1 & 0 \\ 0 & -1 \end{pmatrix}, \qquad \gamma^1 = \mathrm{i}\sigma_2 = \begin{pmatrix} 0 & 1 \\ -1 & 0 \end{pmatrix}, \tag{2}$$

$\bar\Psi = (\Psi^\star)^\intercal\,\gamma^0$ is the Dirac adjoint spinor, ρ is the dissipation coefficient, and the term $f(x)\Psi^\star$ represents the parametric force. Notice that a damping term $-\mathrm{i}\rho\Psi$ would not be correct. The NLD equation with a real potential $V(x)$ would have a term $V(x)\,\gamma^0\,\Psi$ [25]. An imaginary potential produces damping, so the simplest choice to introduce the dissipation is with an imaginary constant $-\mathrm{i}\rho$.

In this work, as was mentioned in the Introduction, we will focus on a spatially periodic force

$$f(x) = r\cos(K\,x)\,, \tag{3}$$

with amplitude r and wave number K.

The corresponding damped parametrically driven adjoint NLD equation is

$$\mathrm{i}\partial_\mu\bar\Psi\gamma^\mu + m\bar\Psi - g^2(\bar\Psi\Psi)\bar\Psi = -f^\star(x)\bar\Psi^\star - \mathrm{i}\,\rho\,\bar\Psi\,\gamma^0\,. \tag{4}$$

The equations (1) and (4) can be derived in a standard fashion from the Lagrangian density

$$\mathcal{L} = \left(\frac{\mathrm{i}}{2}\right)[\bar\Psi\gamma^\mu\partial_\mu\Psi - \partial_\mu\bar\Psi\gamma^\mu\Psi] - m\bar\Psi\Psi + \frac{g^2}{2}(\bar\Psi\Psi)^2 - \frac{1}{2}f\bar\Psi\Psi^\star - \frac{1}{2}f^\star\bar\Psi^\star\Psi, \tag{5}$$

and from the dissipation function

$$\mathcal{F} = -\mathrm{i}\,\rho\,(\bar\Psi\gamma^0\partial_t\Psi - \partial_t\bar\Psi\gamma^0\Psi). \tag{6}$$

Indeed, inserting (5) and (6) into the generalized Euler–Lagrange equations

$$\partial_\mu\frac{\partial\mathcal{L}}{\partial(\partial_\mu\bar\Psi)} - \frac{\partial\mathcal{L}}{\partial\bar\Psi} = \frac{\partial\mathcal{F}}{\partial(\partial_t\bar\Psi)}, \tag{7}$$

$$\partial_\mu\frac{\partial\mathcal{L}}{\partial(\partial_\mu\Psi)} - \frac{\partial\mathcal{L}}{\partial\Psi} = \frac{\partial\mathcal{F}}{\partial(\partial_t\Psi)}, \tag{8}$$

the equations (1) and (4) are obtained, respectively. Notice that some derivatives are subtle. For instance,

$$\frac{\partial}{\partial\bar\Psi}(\bar\Psi\Psi^\star) = \left(\frac{\partial}{\partial\Psi_1^\star}, \quad -\frac{\partial}{\partial\Psi_2^\star}\right)^\intercal[(\Psi_1^\star)^2 - (\Psi_2^\star)^2] = (2\,\Psi_1^\star, \quad 2\,\Psi_2^\star)^\intercal\,.$$

For a soliton solution of the equation (1), the charge is defined as

$$Q = \int_{-\infty}^{+\infty} \mathrm{d}x\, \bar{\Psi}\, \gamma^0\, \Psi. \tag{9}$$

By multiplying equation (1) to the left by $\bar{\Psi}$ and equation (4) to the right by Ψ, adding both expressions and integrating over x, the following evolution equation for the charge is obtained

$$\frac{\mathrm{d}Q}{\mathrm{d}t} = -2\rho Q - \mathrm{i} \int_{-\infty}^{+\infty} \mathrm{d}x\, [f\bar{\Psi}\, \Psi^\star - f^\star \bar{\Psi}^\star\, \Psi], \tag{10}$$

where it has been assumed that $\bar{\Psi}(+\infty,t)\gamma^1\Psi(+\infty,t) - \bar{\Psi}(-\infty,t)\gamma^1\Psi(-\infty,t) = 0$. Therefore, the charge is not conserved. This is an expected result since the Lagrangian is not invariant under the transformation of phase $\Psi \to \mathrm{e}^{\mathrm{i}\,\Lambda}\,\Psi$ [25].

An evolution equation for the momentum of a solitary wave

$$P = \frac{\mathrm{i}}{2} \int_{-\infty}^{+\infty} \mathrm{d}x\, \left(\bar{\Psi}_x\, \gamma^0 \Psi + \bar{\Psi}\, \gamma^0\, \Psi_x\right), \tag{11}$$

can be obtained by multiplying equation (1) to the left by $\bar{\Psi}_x$ and equation (4) to the right by Ψ_x, substracting both expressions and integrating over x. This procedure yields

$$\frac{\mathrm{d}P}{\mathrm{d}t} = -2\,\rho P + \int_{-\infty}^{+\infty} \mathrm{d}x\, [f\bar{\Psi}_x \Psi^\star + f^\star \bar{\Psi}^\star \Psi_x], \tag{12}$$

where it was assumed that the momentum current density

$$T^{11} = -m\,\bar{\Psi}\,\Psi + \frac{g^2}{2}(\bar{\Psi}\Psi)^2 + \frac{\mathrm{i}}{2}\,(\bar{\Psi}\,\gamma^0\Psi_t - \bar{\Psi}_t\,\gamma^0\,\Psi), \tag{13}$$

fullfils $T^{11}(+\infty,t) - T^{11}(-\infty,t) = 0$. Consequently, the momentum is not preserved either due to the dissipation and/or due to the inhomogeneity of the force.

The energy of a soliton solution is

$$E(t) = \int_{-\infty}^{+\infty} \mathrm{d}x\, T^{00}, \tag{14}$$

where the energy density reads

$$\begin{aligned} T^{00} &= \frac{\mathrm{i}}{2}(\bar{\Psi}\,\gamma^0\Psi_t - \bar{\Psi}_t\,\gamma^0\,\Psi) - \mathcal{L} \\ &= -\left(\frac{\mathrm{i}}{2}\right)[\bar{\Psi}\gamma^1\Psi_x - \bar{\Psi}_x\gamma^1\Psi] + m\bar{\Psi}\Psi - \frac{g^2}{2}(\bar{\Psi}\Psi)^2 + \frac{f(x)}{2}\bar{\Psi}\Psi^\star + \frac{f^\star(x)}{2}\bar{\Psi}^\star\Psi. \end{aligned} \tag{15}$$

By multiplying equation (1) to the left by $\bar{\Psi}_t$ and equation (4) to the right by Ψ_t, substracting both expressions, integrating over x, and assuming that $T^{10}(+\infty,t) - T^{10}(-\infty,t) = 0$, being $T^{10} = \frac{\mathrm{i}}{2}\,(\bar{\Psi}\,\gamma^1\Psi_t - \bar{\Psi}_t\,\gamma^1\,\Psi)$ the energy current density, we get the following evolution equation for the energy

$$\frac{\mathrm{d}E}{\mathrm{d}t} = \int_{-\infty}^{+\infty} \mathrm{d}x\, \mathcal{F}. \tag{16}$$

Therefore, only in the non-dissipative case, $\rho = 0$, the energy will be conserved.

3. Collective coordinates ansatz

The aim of this section is to find an approximate solution of equation (1). A standard procedure in perturbed extended models supporting soliton solutions is to assume that the approximate solution has the same functional form as the exact solution [9, 11, 12, 26]. Moreover, this solution will depend on time only through the so-called collective coordinates. Specifically, for the NLD equation without perturbation, i.e. equation (1) with $\rho = 0$ and $f(x) = 0$, the two spinor components of a moving soliton solution are given by

$$\begin{aligned}\Psi_1(x,t) &= \mathrm{e}^{-\mathrm{i}\omega t'}\left\{\cosh\left[\frac{\eta}{2}\right]A(x') + \mathrm{i}\sinh\left[\frac{\eta}{2}\right]B(x')\right\},\\ \Psi_2(x,t) &= \mathrm{e}^{-\mathrm{i}\omega t'}\left\{\sinh\left[\frac{\eta}{2}\right]A(x') + \mathrm{i}\cosh\left[\frac{\eta}{2}\right]B(x')\right\},\end{aligned} \tag{17}$$

where $x' = \gamma(x - vt)$, $t' = \gamma(t - vx)$, and

$$A(x') = \frac{\sqrt{2}\beta}{g}\frac{\sqrt{m+\omega}\cosh(\beta x')}{m+\omega\cosh(2\beta x')}, \tag{18}$$

$$B(x') = \frac{\sqrt{2}\beta}{g}\frac{\sqrt{m-\omega}\sinh(\beta x')}{m+\omega\cosh(2\beta x')}. \tag{19}$$

In the above equations ω is a constant frequency, $\gamma = \cosh(\eta) = 1/\sqrt{1-v^2}$ is the Lorentz factor, η is the rapidity, and $\beta = \sqrt{m^2-\omega^2}$.

In order to look for an approximate soliton solution of the damped parametrically driven NLD equation (1) with (3), we assume that, due to the smallness of the perturbation, the only modification to the exact solutions (17) of the NLD equation is that the constant parameters become time dependent functions. This implies that in equations (17)–(19) we replace

$$vt \to q(t);\ \omega \to \omega(t);\ \eta \to \eta(t);\ \ \omega t' = \gamma\omega(t - vx) \to \phi(t) - p(t)[x - q(t)]. \tag{20}$$

Thus, our trial wave function, with the five collective coordinates $q(t)$, $\omega(t)$, $\eta(t)$, $\phi(t)$ and $p(t)$, reads

$$\psi_{1a}(x,t) = \mathrm{e}^{-\mathrm{i}\phi(t)+\mathrm{i}p(t)[x-q(t)]}\left\{\cosh\left[\frac{\eta(t)}{2}\right]A(x,t) + \mathrm{i}\sinh\left[\frac{\eta(t)}{2}\right]B(x,t)\right\}, \tag{21}$$

$$\psi_{2a}(x,t) = \mathrm{e}^{-\mathrm{i}\phi(t)+\mathrm{i}p(t)[x-q(t)]}\left\{\sinh\left[\frac{\eta(t)}{2}\right]A(x,t) + \mathrm{i}\cosh\left[\frac{\eta(t)}{2}\right]B(x,t)\right\}, \tag{22}$$

where $\beta(t) = \sqrt{m^2-\omega^2(t)}$ and $A(x,t)$ and $B(x,t)$ are given by

$$A(x,t) = \frac{\sqrt{2}\beta(t)}{g}\frac{\sqrt{m+\omega(t)}\cosh\{\beta(t)[x-q(t)]\cosh[\eta(t)]\}}{m+\omega(t)\cosh\{2\beta(t)[x-q(t)]\cosh[\eta(t)]\}}, \tag{23}$$

$$B(x,t) = \frac{\sqrt{2}\beta(t)}{g}\frac{\sqrt{m-\omega(t)}\sinh\{\beta(t)[x-q(t)]\cosh[\eta(t)]\}}{m+\omega(t)\cosh\{2\beta(t)[x-q(t)]\cosh[\eta(t)]\}}. \tag{24}$$

This ansatz implies that $q(t)$ is the position of the mass center of the soliton, while $\eta(t)$ and $\omega(t)$ determine the width and the height of the soliton. The other two collective coordinates are used for consistency with the exact solution of the unperturbed NLD equation [21]. A similar ansatz was considered in [25] where the dynamics of the soliton under linear, harmonic and

periodic potentials was investigated. However, due to the conservation of the charge for these perturbations, the frequency was not considered as a collective coordinate.

In order to obtain the equations of motion of the collective variables, we insert (21) and (22) into (5) and (6), and integrate over x. After cumbersone calculations, the following Lagrangian is obtained

$$L = Q_a[\omega(t)]\left\{p(t)\dot{q}(t) + \dot{\phi}(t) - p(t)\,\tanh[\eta(t)]\right\} - I_0[\omega(t)]\{\cosh[\eta(t)] - \dot{q}(t)\sinh[\eta(t)]\} - \frac{\omega(t)\,Q_a[\omega(t)]}{\cosh[\eta(t)]} - U[\omega(t), p(t), q(t), \phi(t), \eta(t)], \tag{25}$$

and the dissipation function

$$F(t) = -2\rho\{Q_a[\omega(t)]\,p(t) + I_0[\omega(t)]\sinh[\eta(t)]\}\dot{q}(t) - 2\rho Q_a[\omega(t)]\dot{\phi}(t) \tag{26}$$

where

$$Q_a[\omega(t)] = \frac{2\,\beta(t)}{g^2\,\omega(t)}, \tag{27}$$

represents the ansatz approximation for the charge,

$$I_0[\omega(t)] = M_0[\omega(t)] - \omega(t)Q_a[\omega(t)], \tag{28}$$

$$M_0[\omega(t)] = \frac{4\,m}{g^2}\,\text{artanh}\{\alpha[\omega(t)]\}, \tag{29}$$

$$\alpha[\omega(t)] = \sqrt{\frac{m-\omega(t)}{m+\omega(t)}}, \tag{30}$$

and all the Lagrangian dependence on q has been collected in the potential $U[\omega(t), p(t), \phi(t), \eta(t), q(t)]$ given by

$$U = \frac{r\,\pi\,Q_a[\omega(t)]}{2\cosh[\eta(t)]}\sum_{n=1}^{2}\frac{a_n(t)\cos[2\,\phi(t) + (-1)^n Kq(t)]}{\sinh[a_n(t)\pi]}\,\cos\left[a_n(t)\,\text{arcosh}\left(\frac{m}{\omega(t)}\right)\right], \tag{31}$$

with

$$a_1(t) = \frac{2\,p(t) + K}{2\,\beta(t)\,\cosh[\eta(t)]}, \tag{32}$$

$$a_2(t) = \frac{2\,p(t) - K}{2\,\beta(t)\,\cosh[\eta(t)]}. \tag{33}$$

From the Lagrange equations

$$\frac{\mathrm{d}}{\mathrm{d}t}\frac{\partial L}{\partial \dot{Y}_i} - \frac{\partial L}{\partial Y_i} = \frac{\partial F}{\partial \dot{Y}_i}, \qquad i = 1, \cdots, 5; \tag{34}$$

we obtain for $Y_1 = q(t)$

$$\frac{\mathrm{d}P_q}{\mathrm{d}t} = -2\rho P_q(t) - \frac{\partial U}{\partial q}, \tag{35}$$

where P_q is the canonical momentum

$$P_q(t) = \frac{\partial L}{\partial \dot{q}} = Q_a[\omega(t)]\, p(t) + I_0[\omega(t)]\, \sinh[\eta(t)]. \tag{36}$$

Notice that equation (35) can be interpreted as the second Newton law for a particle with momentum P_q.

For $Y_2 = p(t)$, the Lagrange equation reads

$$\dot{q}(t) = \tanh[\eta(t)] + \frac{1}{Q_a[\omega(t)]} \frac{\partial U}{\partial p}. \tag{37}$$

Setting $Y_3 = \omega(t)$ in (34) and taking into account (37), we get

$$\dot{\phi}(t) = \frac{\omega(t)}{\cosh[\eta(t)]} - \left(\frac{\omega(t)\beta^2(t)}{m^2 Q_a[\omega(t)]}\right) \left\{ \left(\frac{m^2 p(t)}{\omega(t)\beta^2(t)} + \sinh[\eta(t)] \right) \frac{\partial U}{\partial p} + \frac{\partial U}{\partial \omega} \right\}. \tag{38}$$

For the phase $Y_4 = \phi(t)$, the corresponding Lagrange equation reads

$$\dot{\omega}(t) = \frac{\beta^2(t)\omega(t)}{m^2} \left(2\rho + \frac{1}{Q_a[\omega(t)]} \frac{\partial U}{\partial \phi} \right). \tag{39}$$

Finally, with $Y_5 = \eta(t)$ and taking into account equation (37), we obtain that the five collective coordinates $\phi(t)$, $\omega(t)$, $\eta(t)$, $p(t)$ and $q(t)$ must satisfy the following algebraic equation

$$[\omega(t)\sinh[\eta(t)] - p(t)] \frac{Q_a[\omega(t)]}{\cosh^2[\eta(t)]} + \frac{I_0[\omega(t)]}{Q_a[\omega(t)]} \cosh[\eta(t)] \frac{\partial U}{\partial p} = \frac{\partial U}{\partial \eta}. \tag{40}$$

Therefore, the equations (35), (37)–(40) constitute a set of four ordinary differential equations and one algebraic equation. In order to solve them numerically, the initial values of four collective coordinates have to be specified. For instance, setting $q(0)$, $\eta(0)$, $\omega(0)$ and $\phi(0)$, the initial condition for $p(0)$ is determined by solving the algebraic equation (40). Once all the initial values have been fixed, the equations of motion (35), (37)–(40) can be solved by a Mathematica program.

It is interesting to note that the five equations (35), (37)–(40) for the collective coordinates can be derived using an alternative method, namely the method of moments. By inserting the ansatz (21) and (22) in the evolution equation for the charge (10), equation (39) is obtained. Similarly, inserting the ansatz in the evolution equations for the momentum (12) and the energy (16) leads to (35) and to (38) and (40), respectively. Finally, equation (37) can be deduced in the same way from a dynamical equation for the first moment of the charge

$$Q_1(t) = \int_{-\infty}^{+\infty} \mathrm{d}x\, x\, (\bar{\Psi}\, \gamma^0 \Psi). \tag{41}$$

4. Numerical simulations

In this section the soliton dynamics of the damped parametrically driven NLD equations (1) with (3) is studied by means of simulations. We use a Runge–Kutta–Verner fifth-order algorithm with variable time step and a spectral method for computing the spatial derivatives [27]. The system has been discretized taking constant spacial interval $\Delta x = 0.02$ and a number of points $N = 3200$. Therefore the length of the system is $L = N\Delta x = 64$. Periodic boundary conditions imply that L has to be an integer multiple of the spatial period $\lambda = 2\pi/K$. Additionally λ has to be conmensurable with Δx. As a consequence, the values of the wavenumber K used

in the simulations are restricted to the discrete set $K_n = n\pi/32$, where n is a multiple of 2 or 5. In all simulations we have fixed $m = 1$ and $g = 1$. As initial condition the equations (21) and (22) have been used by specifying the initial values of $q(0)$, $\eta(0)$, $\omega(0)$, $\phi(0)$ and $p(0)$, i.e.

$$\psi_1(x,0) = \mathrm{e}^{-\mathrm{i}\phi(0)+\mathrm{i}p(0)[x-q(0)]}\left(\cosh\left[\frac{\eta(0)}{2}\right]A(x,0) + \mathrm{i}\sinh\left[\frac{\eta(0)}{2}\right]B(x,0)\right), \tag{42}$$

$$\psi_2(x,0) = \mathrm{e}^{-\mathrm{i}\phi(0)+\mathrm{i}p(0)[x-q(0)]}\left(\sinh\left[\frac{\eta(0)}{2}\right]A(x,0) + \mathrm{i}\cosh\left[\frac{\eta(0)}{2}\right]B(x,0)\right), \tag{43}$$

where $A(x,0)$ and $B(x,0)$ represent the functions (23) and (24) evaluated at $t = 0$, respectively.

In order to plot the time evolution of the center of mass of the soliton, we have computed the normalized first moment of the charge, i.e. $Q_1(t)/Q(t)$, which in the collective coordinates approximation agrees with the position $q(t)$. Additionally, by using (9), (11), and (14) we have also computed the time evolution of the charge, the momentum and the energy. These magnitudes are compared with the approximations (27) and (36) for the charge and the momentum, and with the following expression for the energy

$$E_a(t) = P_q(t)\tanh[\eta(t)] + \frac{M_0[\omega(t)]}{\cosh[\eta(t)]} + U[\omega(t), p(t), \phi(t), \eta(t), q(t)], \tag{44}$$

which has been obtained inserting the ansatz (21) and (22) in (14).

4.1. Non-dissipative case

Let us begin considering the non-dissipative case, $\rho = 0$, for which the energy of the soliton is a conserved quantity, as was mentioned in section 2. As initial conditions, we have always taken $q(0) = 0$ for the initial position of the soliton center, $\omega(0) = 0.9$ and $\phi(0) = 0$. We have varied $\eta(0)$ and the parameters of the parametric force r and K, since the initial value $p(0)$ is determined by the algebraic equation (40).

To start with, the simplest choice is taking $K = 0$ which means that the parametric force f is constant. In this case, the potential U loses its dependence on q, therefore $\frac{\partial U}{\partial q} = 0$, and according to equation (35) the momentum P_q becomes constant. If we additionally fix $\eta(0) = 0$, then $p(0) = 0$, and according to equation (36), $P_q = 0$, i.e. the soliton does not move and remains at rest. Consequently, the presence of a force is not a sufficient condition to generate soliton motion. Although the soliton does not move, its charge $Q(t)$ oscillates in time with the frequency $2\omega(0)$ due to its dependence on $\omega(t)$. This is shown in figure 1 for the static soliton corresponding to $K = 0$ and $r = 0.02$. The exact simulation result of the NLD equation and the collective coordinate approximation (27) superimpose and are indistinguishable. In fact, there are static soliton solutions for $q(0) = 0$, $\eta(0) = 0$, $p(0) = 0$ and any value of K. These static solitons correspond to solutions of the collective coordinate system of equations with $q(t) = 0$, $\eta(t) = 0$, and $p(t) = 0$. In this case, the remaining collective variables $\omega(t)$ and $\phi(t)$ satisfy

$$\dot{\phi}(t) = \omega(t) - \frac{\omega(t)\beta^2(t)}{m^2 Q_a[\omega(t)]}\frac{\partial \tilde{U}}{\partial \omega} \tag{45}$$

$$\dot{\omega}(t) = \frac{\beta^2(t)\omega(t)}{m^2}\left(2\rho + \frac{1}{Q_a[\omega(t)]}\frac{\partial \tilde{U}}{\partial \phi}\right), \tag{46}$$

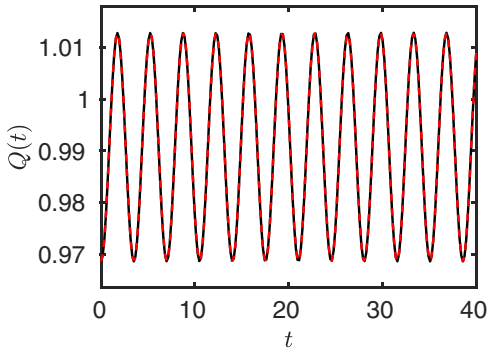

Figure 1. Oscillation of the soliton charge for a static soliton with $K = 0$, $r = 0.02$ and $\rho = 0$. The simulation of the NLD equation (1) (black solid line) and the collective coordinate theory (red dashed line) superimpose. The frequency of the oscillations is approximately $2\omega(0)$. Initial conditions: $q(0) = 0$, $\omega(0) = 0.9$, $\phi(0) = 0$, $\eta(0) = 0$, and $p(0) = 0$.

where $\tilde{U}[\omega(t), \phi(t)] = U[\omega(t), 0, \phi(t), 0, 0]$.

If $K = 0$ but $\eta(0) \neq 0$, the soliton receives an initial impulse $P_q(0) \neq 0$ and moves almost uniformly, as it is shown in figure 2. There are very small ripples of frequency $2\omega(0)$ that can be appreciated in the inset where we have represented $q(t) - \bar{v}t$ versus time, being $\bar{v} \simeq 0.097$ the average velocity. The agreement between the simulation result of the NLD equation and the collective coordinate approximation is excellent. The charge of the soliton oscillates again with frequency $2\omega(0)$ as in figure 1.

For $K \neq 0$ there appears a competition between two length scales: the width of the soliton, which for the used parameters is $l_s \sim 8$ dimensionless units, and the spatial period of the parametric force $\lambda = 2\pi/K$. When $\lambda \gg l_s$, i.e. $K \ll 1$, the soliton oscillates inside an effective potential. In figure 3, from top to bottom, the oscillations of the soliton center, the charge and the momentum are shown for $K_1 = \pi/32 \simeq 0.098$ and $r = 0.02$. The simulation results of the NLD equation (1) are plotted as black continuous lines while the collective variable approximation is represented by red dashed lines. For short times both are indistinguishable but for long times deviations appear. Notice the presence of two very different frequencies. There are very slow and large oscillations of frequency $\Omega_K \simeq 0.002$ with approximately 5 units of the amplitude in $q(t)$. Moreover, there are very fast and small oscillations of frequency $2\omega(0)$, clearly visible in the insets of the panels. In the simulations, the amplitudes of these fast oscillations vary in time. For instance in the top panel the black line is thicker in the interval $500 < t < 2500$, indicating larger fast oscillations. This feature is not captured by the collective coordinate approximation, whose fast oscillations have very small amplitudes not visible in the scale of the inset.

Interestingly, the small frequency Ω_K does not appear in the collective coordinate approximation for the charge. The early time oscillations of Q_a around 0.99, shown in the inset of the middle panel of figure 3, persist for long time. The large increase of Q observed in the simulations is an indication of the presence of soliton instabilities [28].

In the opposite limit $\lambda \ll l_s$ and therefore $K \gg 1$. In this limit the potential U (see equation (31)) vanishes and the soliton moves as a free particle with constant charge, energy and momentum, i.e. the soliton moves very similar as for $K = 0$, but without oscillations of the charge. The straight line in figure 4, which corresponds to the case $K_{128} = 4\pi \simeq 12.566$, illustrates this limit, which is well captured by the collective coordinates approach.

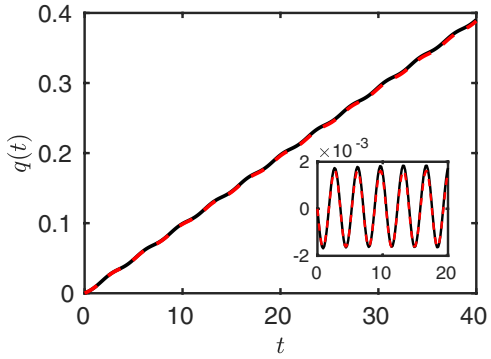

Figure 2. Time evolution of the soliton center for $K = 0$, $r = 0.02$ and $\rho = 0$. The simulation of the NLD equation equation (1), represented by a black solid line, and the collective coordinate approximation, plotted with a red dashed line superimpose. The energy and the momentum are constant. Initial conditions: $q(0) = 0$, $\omega(0) = 0.9$, $\phi(0) = 0$, $\eta(0) = 0.01$, and $p(0) \simeq 0.008\,986$.

In the intermediate case when $\lambda \sim l_s$, the transition between oscillations and uniform motion takes place. Once the initial conditions are fixed, the precise value of K at which the transition occurs depends on the amplitude r, as is shown in figure 5. In this figure the blank region corresponds to soliton oscillations while the shaded region corresponds to net soliton motion. The continuous line that separates both regions has been computed using the collective coordinates approach, because it allows to vary smoothly the value of K for a fixed amplitude r. For instance, for $r = 0.02$ (see the dashed horizontal line in figure 5), the threshold to net motion is found at $K^* \simeq 0.59$. However, in the simulations of the NLD equation (1), due to the periodic boundary conditions, K can only take the set of discrete values $K_n = n\pi/32$ where n is a multiple of 2 or 5. Oscillations are observed for $K_1 = \pi/32 \simeq 0.098$, $K_2 = \pi/16 \simeq 0.196$ and $K_4 = \pi/8 \simeq 0.39$ (points A–C in figure 5 respectively). As K increases, the small frequency Ω_K also increases and instabilities become stronger. This last feature is in fact characteristic of the progressive match between the two length scales present in the system [13, 15]. Then even small values of the perturbation amplitude r cause growing alterations of the soliton shape that is finally destroyed. For instance, in the case $K_4 = \pi/8$ the soliton disappears for times of order of 1000. See in figure 6 the fast increase of the soliton charge density reflecting the existence of instabilities. In the collective coordinate approximation the charge oscillates with constant amplitude around its initial value. Therefore, these instabilities are not predicted by the collective coordinate approach.

Net soliton motion appears in the simulations for $K_5 = 5\pi/32$ (point D in figure 5), which is the closest possible value to K^*. The evolution of the soliton center and the soliton charge corresponding to this case have been plotted in figure 7. In the bottom panel, the persistence of both the slow and the fast oscillations can be clearly appreciated. The instabilities also persist as the large growth of the charge indicates. For larger K they become weaker as the wavelength of the perturbation ceases to match the width of the soliton. But even in the case $K_{128} = 4\pi$ (out of the range of figure 5 and plotted in figure 4), weak instabilities remain and destroy the soliton for long times.

The above scenario is similar to the one described in [16–18] for other localized structures as kinks or breathers in φ^4 or sine-Gordon systems.

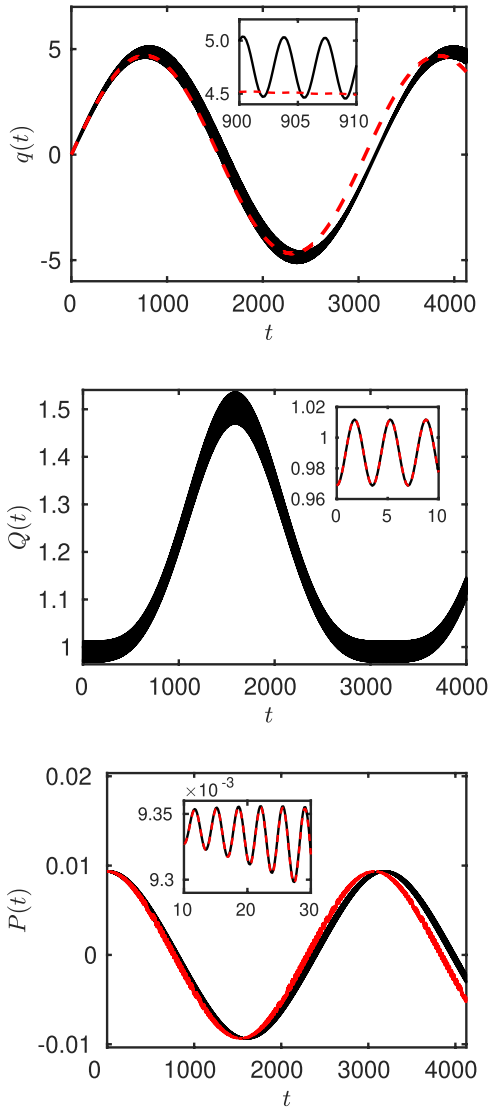

Figure 3. Oscillations in time of the soliton center (top panel), its charge (middle panel) and its momentum (bottom panel) for $K_1 = \pi/32$, $r = 0.02$ and $\rho = 0$. The black continuous lines represent simulations of the NLD equation (1) while the dashed red lines correspond to the collective coordinates approximation. The insets show the existence of very fast oscillations of frequency $2\omega(0)$. Initial conditions: $q(0) = 0$, $\omega(0) = 0.9$, $\phi(0) = 0$, $\eta(0) = 0.01$, and $p(0) \simeq 0.008\,991$.

4.2. Dissipative case

When dissipation is introduced, the soliton charge goes to zero and the soliton disappears in all the range of parameters explored, even for very small values of the damping coefficient ρ. As an example, see the decay of Q in figure 8 for $K_4 = \pi/32$, $r = 0.02$ and $\rho = 0.01$.

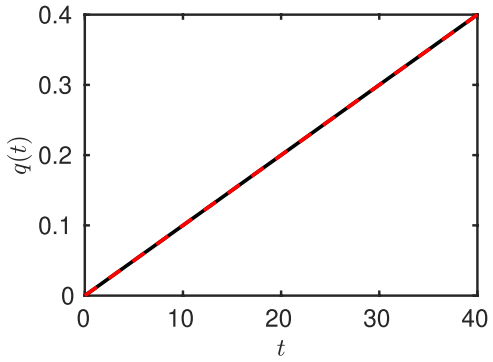

Figure 4. Time evolution of the soliton center for $K_{128} = 4\pi$, $r = 0.02$ and $\rho = 0$. The simulation result of the NLD equation (1), represented by a black solid line, and the collective coordinate approximation, plotted with a red dashed line, superimpose and are indistinguishable. Initial conditions: $q(0) = 0$, $\omega(0) = 0.9$, $\phi(0) = 0$, $\eta(0) = 0.01$, and $p(0) = 0.009$.

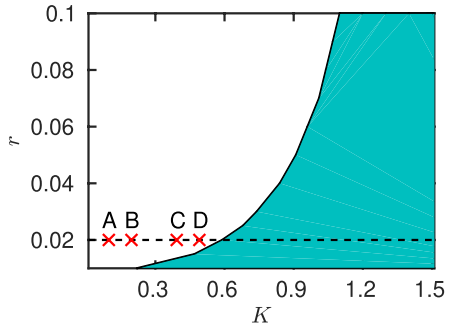

Figure 5. Transition from oscillations (blank region) to soliton net motion (shaded region). This result has been obtained using the collective coordinates theory for the initial conditions: $q(0) = 0$, $\omega(0) = 0.9$, $\phi(0) = 0$, $\eta(0) = 0.01$. For $r = 0.02$ and $\rho = 0$ (dashed line) the transition occurs at $K^\star \simeq 0.59$. In the simulations, due to the discretization and the periodic boundary conditions, the possible values of the wavenumber $K < K^\star$ are restricted to $K_1 = \pi/32, K_2 = \pi/16, K_4 = \pi/8$ and $K_5 = 5\pi/32$ (points A–D, respectively).

The collective coordinate theory again fits very well to the simulations of the NLD equation (1). We have not been able to find out parameter values for which a balance between energy losses and gains leads to soliton survival. This result can be understood taking into account that in the collective coordinate description $\omega = 1$ becomes an attractor of the dynamics when $\rho \neq 0$. If $\omega \to 1$ then $\beta(t) \to 1$, $M_0(t) \to 0$, $I_0(t) \to 0$ and, consequently, it is easy to check that the charge Q_a, the momentum P_q and the energy E_a go to zero, with the only assumption that the collective variables $\eta(t)$ and $p(t)$, and the time derivatives $\dot{q}(t)$ and $\dot{\phi}(t)$, are all bounded functions.

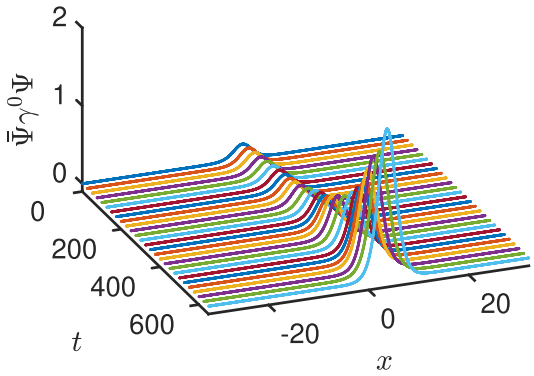

Figure 6. Spatial profiles of the charge density at fixed values of time. Results obtained from numerical simulations of equation (1) for $K_4 = \pi/8$, $r = 0.02$ and $\rho = 0$. The wavelength and the soliton width are of the same order causing an early appearance of instability. Initial conditions: $q(0) = 0$, $\omega(0) = 0.9$, $\phi(0) = 0$, $\eta(0) = 0.01$ and $p(0) = 0.009$.

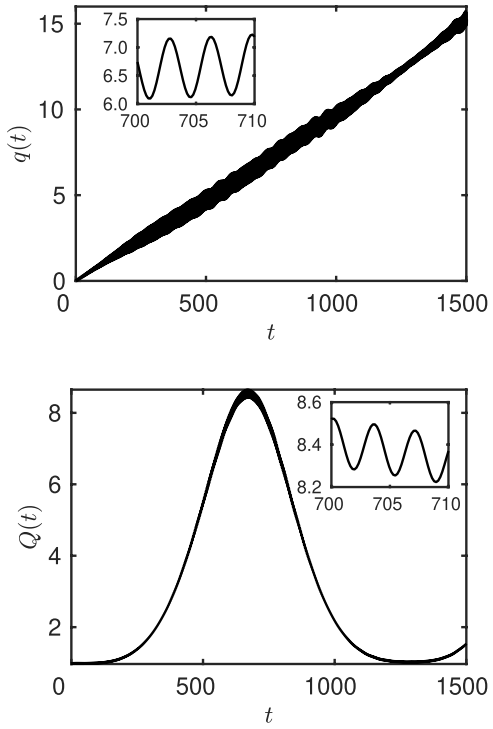

Figure 7. Simulation of the NLD equation (1) for $K = 5\pi/32$, and $r = 0.02$. The top panel shows the net motion of the soliton center while in the bottom panel the time evolution in time of the charge is plotted. The insets show the existence of fast oscillations of frequency $2\omega(0)$. Initial conditions: $q(0) = 0$, $\omega(0) = 0.9$, $\phi(0) = 0$, $\eta(0) = 0.01$, and $p(0) \simeq 0.008\,991$.

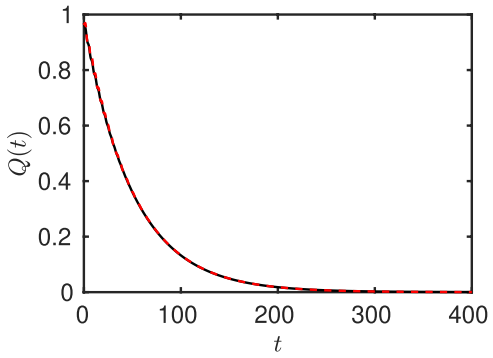

Figure 8. Time evolution of the charge in the dissipative case with $\rho = 0.01$, $K = \pi/8$ and $r = 0.02$. The simulation of the NLD equation (1) (black solid line) and the collective coordinate theory (red dashed line) superimpose. Initial conditions: $q(0) = 0$, $\omega(0) = 0.9$, $\phi(0) = 0$, $\eta(0) = 0.01$ and $p(0) = 0.009$.

5. Summary

Solitary waves of the NLD equation in $1 + 1$ dimensions with scalar–scalar self-interaction, a damping term and parametric driving of the form $r\cos(Kx)$ have been considered. The dynamics of the solitons depends crucially on the length-scale competition between the spatial period $\lambda = 2\pi/K$ of the force and the soliton width l_s. For $\lambda \gg l_s$ the soliton performs oscillations in an effective potential, while for $\lambda \ll l_s$ it moves uniformly as a free particle with constant charge, momentum and energy. In the transition region between the two regimes the soliton is destabilized and is eventually destroyed.

The above results were obtained in two ways: simulations, i.e. numerical solutions of the driven and damped NLD equation, and a variational approach using an ansatz with five collective coordinates which results in four ODEs plus one algebraic equation, which are solved numerically using a Mathematica program. This system of equations is also derived by using the so-called method of moments [21, 29]. For $K = 0$, zero initial rapidity and no damping, the soliton does not move, but its charge Q oscillates with the frequency $2\omega(0)$, where $\omega(t)$ is one of the collective coordinates. For $K = 0$ and finite initial rapidity all collective coordinates oscillate. The soliton position oscillates around a straight line $\bar{v}t$, where $\bar{v}$ is an average velocity. In both cases, simulation and theory agree perfectly.

For $\lambda \gg l_s$ and finite initial rapidity, the soliton moves inside an effective potential and exhibits two very different frequencies: there are very slow oscillations with a large amplitude and very fast oscillations with a small amplitude. For short times the simulation and collective coordinate results are indistinguishable, but for very long times small deviations occur. However with one exception: the collective coordinate result for the charge Q does not show the very slow oscillation with large amplitude. The reason is that Q depends only on one collective coordinate, namely $\omega(t)$ in which the slow frequency is absent. For $\lambda \ll l_s$ the soliton moves as a free particle with constant charge, momentum and energy, which is well captured by the collective coordinate approach.

If λ is in the order of l_s, the collective coordinate theory yields a curve in the space of the parameters r and K which separates the oscillatory region from the region of uniform motion. In the former region the simulations show that the soliton becomes unstable the closer it is to the above transition curve. These instabilities are not predicted by the collective coordinate approach.

In the dissipative case when ρ is nonzero, the charge Q goes to zero and the soliton vanishes eventually. Here, simulations and collective coordinate theory agree perfectly. We did not find values for the parameters and initial conditions for which there is a balance between energy losses and gains.

As a final remark, let us to point out the possibility of studying modulations of parameters of the NLD equation such as the nonlinear coupling constant. This modulation could be able to stabilize the soliton dynamics. This issue has already been investigated in the context of the NLS equation (see, for instance, [30, 31]).

Acknowledgments

FGM acknowledges financial support and hospitality of the University of Seville. NRQ acknowledges the financial support from the Alexander von Humboldt Foundation and the hospitality of the Physikalisches Institut at the University of Bayreuth (Germany) and financial support from the Ministerio de Economía y Competitividad of Spain through FIS2017-89349-P.

ORCID iDs

Niurka R Quintero https://orcid.org/0000-0003-3503-3040
Bernardo Sánchez-Rey https://orcid.org/0000-0003-3170-154X
Franz G Mertens https://orcid.org/0000-0002-0574-2279

References

[1] Drazin P G and Johnson R S 1989 *Solitons: an Introduction* (Cambridge: Cambridge University Press)
[2] Dauxois Th and Peyrard M 2006 *Physics of Solitons* (Cambridge: Cambridge University Press)
[3] Scott A C 1999 *Nonlinear Science* (Oxford: Oxford University)
[4] Kivshar Y S and Malomed B A 1989 Dynamics of solitons in nearly integrable systems *Rev. Mod. Phys.* **61** 763
[5] Rietmann M, Carretero-González R and Chacón R 2011 Controlling directed transport of matter-wave solitons using the ratchet effect *Phys. Rev.* A **83** 053617
[6] Nogami Y, Toyama F M and Zhao Z 1995 Nonlinear Dirac soliton in an external field *J. Phys. A: Math. Gen.* **28** 1413
[7] Salerno M and Zolotaryuk Y 2002 Soliton ratchetlike dynamics by ac forces with harmonic mixing *Phys. Rev.* E **65** 056603
[8] Morales-Molina L, Quintero N R, Sánchez A and Mertens F G 2006 Soliton ratchets in homogeneous nonlinear Klein–Gordon systems *Chaos* **16** 013117
[9] Yershov K V, Kravchuk V P, Sheka D D and Gaididei Y 2016 Curvature and torsion effects in spin-current driven domain wall motion *Phys. Rev.* B **93** 094418
[10] Quintero N R, Mertens F G, Efimov A and Bishop A R 2016 Soliton dynamics in optical fibers using the generalized traveling-wave method *Phys. Rev.* E **93** 042214
[11] Morales-Molina L, Quintero N R, Mertens F G and Sánchez A 2003 Internal mode mechanism for collective energy transport in extended systems *Phys. Rev. Lett.* **91** 234102
[12] Yershov K V, Kravchuk V P, Sheka D D, Pylypovskyi O V, Makarov D and Gaididei Y 2018 Geometry-induced motion of magnetic domain walls in curved nanostripes *Phys. Rev.* B **98** 060409
[13] Sánchez A and Bishop A R 1998 Collective coordinates and length-scale competition in spatially inhomogeneous soliton-bearing equations *SIAM Rev.* **40** 579

[14] Sánchez A, Bishop A R and Domínguez-Adame F 1994 Kink stability, propagation, and length-scale competition in the periodically modulated sine-Gordon equation *Phys. Rev.* E **49** 4603
[15] Scharf R and Bishop A R 1993 Length-scale competition for the one-dimensional nonlinear Schrödinger equation with spatially periodic potentials *Phys. Rev.* E **47** 1375
[16] Cuenda S and Sánchez A 2005 Length scale competition in nonlinear Klein–Gordon models: a collective coordinate approach *Chaos* **15** 023502
[17] Scharf R, Kivshar Y S, Sánchez A and Bishop A R 1992 Sine-Gordon kink-antikink generation on spatially periodic potentials *Phys. Rev.* A **45** R5369
[18] Sánchez A, Scharf R, Bishop A R and Vázquez L 1992 Sine-Gordon breathers on spatially periodic potentials *Phys. Rev.* A **45** 6031
[19] Mertens F G, Cooper F, Quintero N R, Shao S, Khare A and Saxena A 2016 Solitary waves in the nonlinear Dirac equation in the presence of external driving forces *J. Phys. A: Math. Theor.* **49** 065402
[20] Mertens F G, Cooper F, Shao S, Quintero N R, Saxena A and Bishop A R 2017 Nonlinear Dirac equation solitary waves under a spinor force with different components *J. Phys. A: Math. Theor.* **50** 145201
[21] Quintero N R, Shao S, Alvarez-Nodarse R and Mertens F G 2019 Externally driven nonlinear Dirac equation revisited: theory and simulations *J. Phys. A: Math. Theor.* **52** 155401
[22] Barashenkov I V, Bogdan M M and Korobov V I 1991 Stability diagram of the phase-locked solitons in the parametrically driven, damped nonlinear Schrödinger equation *Europhys. Lett.* **15** 113
[23] Barashenkov I V, Zemlyanaya E V and Bär M 2001 Traveling solitons in the parametrically driven nonlinear Schrödinger equation *Phys. Rev.* E **64** 016603
[24] Alvarez A and Carreras B 1981 Interaction dynamics for the solitary waves of a nonlinear Dirac model *Phys. Lett.* A **86** 327
[25] Mertens F G, Quintero N R, Cooper F, Khare A and Saxena A 2012 Nonlinear Dirac equation solitary waves in external fields *Phys. Rev.* E **86** 046602
[26] Cuenda S and Sánchez A 2004 Nonlinear excitations in DNA: aperiodic models versus actual genome sequences *Phys. Rev.* E **70** 051903
[27] Cuevas-Maraver J, Kevrekidis P, Saxena A, Cooper F and Mertens F 2015 *Solitary Waves in the Nonlinear Dirac Equation at the Continuum Limit: Stability and Dynamics* (New York: Nova Sciences)
[28] Shao S, Quintero N R, Mertens F G, Cooper F, Khare A and Saxena A 2014 Stability of solitary waves in the nonlinear Dirac equation with arbitrary nonlinearity *Phys. Rev.* E **90** 032915
[29] Pérez-García V M, Torres P J and Montesinos G D 2007 The method of moments for nonlinear Schrödinger equations: theory and applications *SIAM J. Appl. Math.* **67** 990
[30] Torres P J 2014 Modulated amplitude waves with non-trivial phase in quasi-1D inhomogeneous Bose–Einstein condensates *Phys. Lett.* A **378** 3285
[31] Belmonte-Beitia J, Pérez-García V M, Vekslerchik V and Konotop V V 2008 Localized nonlinear waves in systems with time- and space-modulated nonlinearities *Phys. Rev. Lett.* **100** 164102